D-1.3.1 Research on Long-term Changes in Biogeochemical Cycles of Elements in the Oceans based on Chemical Components of Marine Sediments

Contact Person Takejiro Takamatsu
Section Director, Soil Science Section
Water and Soil Environment Division
National Institute for Environmental Studies, Environment Agency
16-2 Onogawa, Tsukuba, Ibaragi 305, Japan
Phone +81-298-50-2469, Fax +81-298-51-4732

Total Budget for FY1993-FY1995 23,100,000 Yen (FY1995; 7,789,000 Yen)

Abstract

Sediment cores collected from the shelf of the Weddell Sea (GC808) and from ca. 3500 m depths of the Weddell Sea (GC801), the Ross Sea (GC1208) and off the Enderby Land (GC1002) in the Antarctic Ocean were analyzed for opal, calcium carbonate, carbon, nitrogen and for 25 major and trace elements by neutron activation analysis. Foraminiferal tests were isolated from calcareous ooze layers of the cores and AMS ^{14}C ages were determined. As the results, opal contents varied remarkably from <2% in the lower part of Core GC1002 to ca. 45% of Core GC808, which correspond to the average accumulation rates of from ca. 0.6 cm/kyr to ca. 200 cm/kyr, respectively. Ba contents showed positive correlation relative to opal contents in each core but the slopes were quite different among the four cores. Relationship between opal and Br showed a linear correlation for the four cores. Based on the AMS ^{14}C ages and opal contents, biological productivity due to diatom increased abruptly at 12 kyr BP in the Weddell Sea. It has been revealed that opal contents as well as Ba and Br contents will become very good proxies of paleoproductivity in the oceans.

Key Words Antarctic Ocean, sediments, AMS ^{14}C ages, productivity, opal, trace elements

1. Introduction

All products of processes occurred in marine environments accumulate on the sea-floor as bottom sediments and sediment cores are the dominant continuous records of marine environments. Major components of marine sediments are: biological products in the surface ocean such as organic matter, opal, and calcium carbonate, authigenic minerals such as iron and manganese oxyhydroxides, lithogenous clay minerals and organic matter carried as run-off and/or as eorian dusts, and anthropogenic heavy metals and organic compounds. The oceans seem to play important roles in the global environmental change for thermal transfers and also for material transfers of green-house effect gases such as carbon dioxide and methane. In order to clarify the roles of the oceans, mechanisms of material cycles and their short-term and long-term changes must be resolved. Mechanisms of biogeochemical cycles of materials in the oceans and their changes are the most important problems to be solved. These processes are also related to the deep ocean circulation.

The purposes of the present study are: to analyze biogenous materials and trace elements of marine sediment cores, to determine ^{14}C ages of these cores by accelerator mass spectrometry (AMS), and to develop a methodology to estimate paleoproductivity using sediment core samples collected from the Antarctic Ocean, where biological productivity is quite high.

2. Materials and Methods

Sediment core samples: Sediment core samples have been collected with a gravity corer during R/V Hakurei-maru cruises in the Antarctic Ocean and stored at 5℃. Sub-samples were taken at every 10 cm and dried at 60℃ for 3 days from the following four core samples (Figs. 1 and 2): GC808 from the shelf of the Weddell Sea (61.0°S, 45.1°W; 376 m deep; 545 cm long), GC801 from the Weddell Sea (60.0°S, 52.3°W; 3328 m deep; 666 cm long), GC1208

from the Ross Sea (68.5°S, 172.5°E; 3605 m deep; 470 cm long), and GC1002 from the Enderby Land Basin (63.8°S, 78.9°E; 3658 m deep; 396 cm long).

Separation of foraminiferal tests: Planctonic and benthic foraminiferal tests were picked up using a moistened writing brush under a microscope after passing through a 63-μm sieve.

AMS ^{14}C age determination: Planctonic foraminiferal tests were washed with diluted hydrochloric acid to remove the surface contamination of ca. 10% in weight and rinsed with Milli-Q water. After drying they were decomposed with phosphoric acid at 60°C and evolved CO_2 gas was purified in a vacuum line and converted to graphite by the Fe-catalytic hydrogen reduction method to form targets (Kitagawa et al., 1993). $^{14}C/^{13}C$ ratios were measured relative to NBS oxalic acid standard (NBS SRM-4990C) with a Tandetron accelerator mass spectrometer at Nagoya University and calculated as conventional ^{14}C ages after correcting the isotope fractionation using $^{13}C/^{12}C$ ratios (Stuiver and Polach, 1977), which were measured with a MAT 252 mass spectrometer using a portion of the CO_2 gas. In Cores GC808 and GC801 from the Weddell Sea calcium carbonate were not found and ^{14}C ages were determined using organic carbon after removing inorganic carbon.

Biogenic amorphous silica (opal): Biogenic amorphous silica (opal) was analyzed after the method of Mortlock and Froelich (1989). About 100 mg of dried sediment sample was taken in a polypropylene test tube and treated with 10% hydrogen peroxide and also with 1M HCl to remove organic matter and calcium carbonate, respectively. After washing and drying, the residue was leached with 2M Na_2CO_3 solution at 85°C by shaking occasionally. A portion of the supernatant solution was sampled at 3 and 5 hours later for the analysis of dissolved silica by the molybdenum yellow method with a flow injection analyzer attached with a autosampler. Opal content was clculated from the 0 hour content, which was estimated from the 3 and 5 hour contents.

Calcium carbonate: Calcium carbonate content was estimated from the calcium content of the hydrogen peroxide plus HCl fraction of opal analysis by atomic absorption spectroscopy.

Carbon and nitrogen: Total carbon and nitrogen were determined with an elemental analyzer.

Neutron activation analysis: Instrumental neutron activation analysis (INNA: Koyama et al., 1987; Masuzawa et al., 1992) was performed using the KUR reactor of Kyoto University for the determination of 25 major and trace elements (Al, V, Mn, Cl, Na, Br, As, Sb, Zn, Co, Cr, Ba, Rb, Cs, Th, Hf, Ta, U, Sc, La, Ce, Sm, Eu, Tb, Yb, and Lu) of sediment samples.

3. Results and Discussion

Table 1 lists opal, calcium carbonate, carbon, nitrogen and 25 major and trace elements in Core GC1208 from the Ross Sea. AMS ^{14}C ages for the four cores were compiled in Fig. 3. Vertical profiles of opal, calcium carbonate, Al, Ba, Br, and U in the four cores were shown in Figs. 4-7.

The Antarctic Ocean is the place of quite high biological productivity due to up-welling of nutrient rich deep waters and the Weddell Sea and Ross Sea are the places of the formation of deep and bottom waters in addition to the northern North Atlantic. Such high biological production is carried out mainly by diatom. Diatom is the dominant component of settling particles (Tsunogai et al., 1986; Fisher et al., 1988) and the bottom surface is covered mainly with diatomaceous ooze.

According to the results of this study, not only opal, calcium carbonate, and organic matter contents but also sedimentation rates showed remarkable differences among the four cores. Opal content of sediments is controlled by the balance between the supplies of opal and lithogenous aluminosilicate. High opal contents indicate very high biological productivity in the surface layer of the oceans, which also control the sedimentation rates. Sedimentation rates varied significantly among the four cores from ca. 0.6 cm/kyr at Core GC1002 from the Enderby Land Basin to ca. 200 cm/kyr at Core GC808 from the shelf of the Weddell Sea (Fig. 3). This order of sedimentation rates is consistent with the order of opal contents. The difference in opal contents between ca. 45% of Core GC808 at 376 m depth and ca. 10% in the upper part of Core GC801 at 3328 m depth in the Weddell Sea suggest the dissolution of opal through sinking and depositing processes.

Ba has been considered to be a good proxy of marine biological productivity (Dymond et al., 1992). Figure 8a plots Ba *vs.* opal in the four cores. Positive correlation between opal and Ba is observed except for Core GC808 but the slopes of Ba *vs.* opal are different among the cores. It is noted that Ba shows no accumulation in Core GC808 where opal contents are quite high. This seems to be important to solve the accumulation mechanism(s) of Ba associating with opal in settling particles and sediments.

Figure 8b shows relationships between opal and Br, which is considered to associate with marine organic matter, in the four cores. Almost all points are plotted along a line throughout the four cores although the points are scattered for Core GC808. This suggests a possibility of Br in settling particles and marine sediments as a useful proxy of biological productivity.

Figure 9 plots the relationships between Al and Th in the four cores. Both Al and Th are lithogenous components (Masuzawa et al., 1989) and Th content reflects the differences in the weathered mother rock(s) supplied to deposited places. Samples of the two cores from the Weddell Sea (Cores GC808 and 801) are plotted along a line, which indicates the mother rock(s) for the two cores were almost the same. The slopes of Th *vs.* Al increase in the order of the Weddell Sea (ca. 0.0012), the Ross Sea (ca. 0.0020), and the Enderby Land Basin (ca. 0.0035). The high Th/Al ratio of the Enderby Land Basin (0.0035) may reflect that Precambrian granitic rocks are dominant in the Enderby Land.

Martin (1990) proposed that biological productivity in the Antarctic Ocean might have been much higher than the present (iron hypothesis). According to the vertical profile of opal in Core GC801 from the Weddell Sea (Fig. 5), it had increased abruptly at 12 kyr BP, that is, after the Last Glacial Period on the contrary to the Martin's hypothesis.

References

Dymond, J., E. Suess and M. Lyle (1992) Barium in deep-sea sediment: a geochemical proxy for paleoproductivity. Paleoceanography, 7, 163-181.

Fischer, G., D. Futterer, R. Gersonde,S. Honjo, D. Ostermann and G. Wefer (1988) Seasonal variability of particle flux in the Weddell Sea and its relation to ice cover. Nature, 335, 426-428.

Kitagawa, H., T. Masuzawa, T. Nakamura and E. Matsumoto (1993) A batch preparation method for graphite targets with low background for AMS ^{14}C measurements. Radiocarbon, 35, 295-300.

Koyama, M., M. Matsushita and J. Takada (1987) Reactor neutron activation analysis by using multi-elemental comparators: problems of nuclear constants of ^{128}I and ^{175}Yb and several other nuclides. J. Radioanal. Nucl. Chem., Articles, 113, 199-207.

Martin, J.H. (1990) Glacial-interglacial CO_2 change: The iron hypothesis. Paleoceanography, 5, 1-13.

Masuzawa, T., S. Noriki, T. Kurosaki, S. Tsunogai and M. Koyama (1989) Compositional change of settling particles with water depth in the Japan Sea. Mar. Chem., 27, 61-78.

Mortlock, R.A. and P.N. Froelich (1989) A simple method for the rapid determination of biogenic opal in pelagic marine sediments. Deep-Sea Res., 36, 1415-1426.

Stuiver, M. and H.A. Polach (1977) Reporting of ^{14}C data. Radiocarbon, 19, 355-363.

Tsunogai, S., S. Noriki, K. Harada, T. Kurosaki, Y. Watanabe and M. Maeda (1986) Large but variable particulate flux in the Antarctic Ocean and its significance for the chemistry of Antarctic water. J. Oceanogr. Soc. Jpn., 42, 83-90.

Table 1. Major and minor chemical composition of Core GC1208 from the Antarctic Ocean.

No.	Depth	Name	Opal	CaCO3	C	N	Al	Fe	Na	Cl	Mn	Br	As	Sb	Zn	Co	Cr	V
	(cm)		(%)	(%)	(%)	(%)	(%)	(%)	(%)	(%)	(ppm)	(ppm)	(ppm)	(ppm)	(ppm)	(ppm)	(ppm)	(ppm)
5-7	60	1	8.33	0.78	0.54	0.09	5.59	4.25	3.09	3.26	1066	120	3.1	0.97	176	19.2	68	83
5-8	70	2	9.30	0.79	0.34	0.06	6.14	4.39	2.59	2.15	1154	73	3.5	0.39	185	19.9	79	116
5-9	80	3	5.33	14.35	1.82	0.04	5.61	3.68	2.23	1.65	906	52	3.2	0.75	141	17.2	58	94
5-10	90	4	5.75	15.73	2.12	0.03	5.81	3.61	2.24	2.12	870	64	3.2	0.60	142	15.4	63	99
4-1	100	5	5.92	6.40	0.74	0.03	5.56	4.02	2.57	2.14	1083	69	3.2	0.93	154	16.4	73	80
4-2	110	6	7.45	1.63	0.24	0.03	5.36	3.36	2.48	1.81	618	52	-	0.40	123	10.4	67	76
4-3	120	7	7.72	0.88	0.10	0.02	4.98	3.48	2.7	1.82	904	57	-	0.51	123	13.7	70	67
4-4	130	8	6.56	1.06	0.18	0.03	5.96	4.02	2.81	2.06	930	68	-	0.93	160	19.6	71	87
4-5	140	9	5.12	4.93	0.70	0.03	5.71	4.34	2.57	1.99	534	70	3.5	0.97	165	18.2	67	77
4-7	160	10	4.43	7.19	0.74	0.04	5.66	4.11	2.46	2.27	520	72	-	0.92	155	18.8	74	97
4-9	180	11	5.19	1.04	0.16	0.03	6.18	4.12	2.42	1.84	1124	61	4.6	0.90	165	20.2	69	76
4-10	190	12	5.73	5.10	0.72	0.03	5.81	3.85	2.47	1.98	999	65	2.8	0.55	154	17.9	65	132
3-1	200	13	4.88	0.72	0.11	0.03	6.19	4.20	2.37	1.61	1249	56	4.3	0.95	156	19.6	76	93
3-2	210	14	5.46	0.64	0.09	0.03	6.07	4.04	2.4	2.01	1183	59	4.3	0.70	154	20.7	78	105
3-3	220	15	5.93	0.62	0.10	0.03	6.11	4.16	2.54	2.11	938	65	3.2	0.75	168	17.9	73	105
3-4	230	16	5.29	0.71	0.11	0.03	5.82	4.10	2.31	1.96	1140	56	3.1	0.84	150	18.1	68	101
3-5	240	17	5.39	0.66	0.08	0.02	5.78	4.09	2.29	1.73	952	54	3.3	0.77	148	19.6	72	99
3-7	260	18	5.95	0.59	0.10	0.03	5.85	3.95	2.41	1.75	878	58	-	1.00	154	17.8	69	95
3-9	280	19	6.47	0.68	0.10	0.02	5.79	3.57	2.27	1.61	691	49	-	0.71	133	13	66	91
3-10	290	20	7.34	0.69	0.10	0.02	6.11	3.41	2.21	1.48	543	49	4.0	0.53	127	12.9	63	74
2-1	300	21	6.92	0.82	0.13	0.02	5.55	3.47	2.19	1.52	575	49	-	-	52	13.8	78	98
2-2	310	22	5.46	1.01	0.10	0.02	6.15	3.94	2.41	1.81	845	55	-	-	142	14.7	64	113
2-3	320	23	6.01	1.68	0.18	0.02	5.44	3.77	2.44	1.51	606	56	-	0.68	140	15.6	65	93
2-4	330	24	4.92	3.97	0.48	0.02	6.29	3.56	2.26	1.61	1274	50	3.9	0.88	181	25.8	65	101
2-5	340	25	6.08	8.76	1.09	0.02	5.41	3.59	2.34	1.72	842	55	-	0.68	142	17.3	65	90
2-7	360	26	5.62	2.51	0.33	0.03	5.63	3.90	2.44	1.66	968	56	4.4	1.02	38	17.9	78	90
2-8	370	27	5.58	1.36	0.19	0.03	5.98	3.74	2.44	1.67	890	60	-	0.89	117	16.8	70	90
2-9	380	28	5.81	0.75	0.09	0.03	5.77	3.75	2.33	1.67	885	51	3.3	0.64	154	14.6	67	92
2-10	390	29	6.91	0.75	0.12	0.02	6.04	3.78	2.42	1.63	716	51	-	0.67	128	14.4	71	98
1-1	400	30	6.95	0.84	0.09	0.03	6.02	3.85	2.42	1.7	753	55	2.6	0.74	160	14.5	76	101
1-2	410	31	6.21	0.88	0.09	0.02	6.42	3.79	2.36	1.74	849	51	-	-	41	14.9	70	101
1-3	420	32	5.65	0.74	0.08	0.02	6.19	3.54	2.24	1.55	910	47	-	0.64	134	16.7	59	111
1-4	430	33	5.68	0.77	0.09	0.03	5.80	3.62	2.43	1.65	918	52	-	0.89	133	18.2	62	95
1-5	440	34	5.78	0.68	0.09	0.03	6.06	3.80	2.45	1.72	806	53	-	0.41	141	16.3	59	88
1-7	460	35	5.39	1.39	0.16	0.03	6.24	3.80	2.43	1.67	950	56	-	0.76	46	17.8	69	107
1-8	470	36	5.50	8.26	0.97	0.03	5.82	3.59	2.42	1.74	753	54	4.9	0.83	139	15.6	57	102
1-9	480	37	5.01	6.47	0.77	0.03	5.73	3.63	2.42	1.79	999	56	3.6	-	117	17.1	78	96
1-10	490	38	6.09	8.80	0.97	0.03	5.59	3.71	2.38	1.75	955	55	-	0.88	169	23.6	65	95
cc-1	500	39	5.52	12.94	1.46	0.02	5.48	3.37	2.26	1.79	853	56	5.9	1.54	-	14.3	73	117
cc-2	510	40	4.63	9.36	1.00	0.02	6.09	3.43	2.38	1.62	958	52	-	0.80	57	16	65	100
cc-3	520	41	4.99	5.29	0.60	0.02	ND	4.08	2.37	ND	ND	56	5.1	1.18	153	21.6	69	ND

Table 1. (continued)

No.	Depth	Name	Ba	Rb	Cs	Th	Hf	Ta	U	Sc	La	Ce	Sm	Eu	Tb	Yb	Lu
	(cm)		(ppm)	(ppm)	(ppm)	(ppm)	(ppm)	(ppm)	(ppm)	(ppm)	(ppm)	(ppm)	(ppm)	(ppm)	(ppm)	(ppm)	(ppm)
5-7	60	1	1350	145	8.8	12.4	5.5	1.84	1.6	12.0	32.2	67	5.4	1.03	0.85	3.1	0.44
5-8	70	2	1690	152	9.3	12.5	5.8	1.98	2.1	12.2	34.6	72	5.9	1.10	0.83	2.6	0.31
5-9	80	3	1190	146	7.4	12.1	6.5	1.65	1.8	9.8	30.9	61	5.4	1.08	0.84	2.2	0.46
5-10	90	4	1150	130	8.4	11.6	5.1	1.67	1.9	10.1	31.1	57	5.4	1.02	0.82	2.5	0.45
4-1	100	5	823	126	8.3	12.2	6.1	2.06	1.9	10.9	34.5	67	6.0	1.17	1.08	2.6	0.60
4-2	110	6	577	97	4.9	10.0	6.8	2.68	2.0	8.5	36.4	68	5.7	1.23	0.91	2.5	0.48
4-3	120	7	580	127	4.2	10.2	7.6	2.79	2.2	8.6	38.6	72	5.7	1.31	0.96	3.2	0.50
4-4	130	8	1120	147	7.9	12.3	7.0	2.69	3.2	10.8	40.0	79	6.8	1.26	1.01	3.1	0.50
4-5	140	9	912	145	9.5	12.8	7.1	2.12	1.9	11.7	34.3	71	6.0	1.15	1.16	1.9	0.53
4-7	160	10	1020	150	9.1	12.0	5.9	1.71	2.5	11.6	31.8	71	5.8	1.11	0.99	2.1	0.44
4-9	180	11	1280	154	9.3	13.7	6.6	1.93	2.1	11.5	35.9	73	6.2	1.11	1.02	2.5	0.54
4-10	190	12	1040	150	8.4	12.0	6.4	2.01	1.9	11.0	33.1	66	5.6	1.05	0.89	3.1	0.43
3-1	200	13	1300	157	9.0	13.3	7.0	1.80	3.0	11.7	37.2	73	6.4	1.17	1.06	3.0	0.57
3-2	210	14	992	158	8.8	13.5	7.3	2.14	3.2	11.6	35.3	71	6.0	1.11	1.11	3.2	0.37
3-3	220	15	1220	151	8.5	12.0	7.0	2.01	2.5	12.5	34.8	69	6.2	1.05	0.89	2.6	0.51
3-4	230	16	1120	146	8.3	12.2	6.5	1.88	2.5	11.3	35.5	69	6.1	1.13	0.91	2.5	0.43
3-5	240	17	1020	163	8.7	12.3	6.4	1.75	2.9	11.5	34.0	68	6.0	1.20	1.00	3.0	0.37
3-7	260	18	946	142	8.8	13.0	6.9	1.84	2.9	11.2	33.3	73	6.0	1.10	0.92	2.5	0.46
3-9	280	19	981	128	6.8	11.7	6.9	1.76	3.0	10.4	33.8	61	5.9	1.05	0.97	3.1	0.54
3-10	290	20	698	145	7.8	12.0	6.2	1.47	2.5	10.1	33.4	63	6.1	1.12	0.83	3.2	0.48
2-1	300	21	681	98	6.9	13.2	6.0	1.47	-	10.2	36.9	65	6.3	1.12	-	3.6	0.64
2-2	310	22	757	135	7.3	11.5	6.9	2.10	2.0	11.0	41.3	71	7.0	1.18	0.63	3.0	0.38
2-3	320	23	701	140	7.5	12.0	6.8	2.15	3.3	10.3	37.9	70	6.5	1.30	1.41	3.5	0.47
2-4	330	24	714	142	8.5	11.7	5.4	1.86	-	9.9	36.9	75	6.8	1.28	-	2.6	0.44
2-5	340	25	961	-	8.0	12.5	7.0	1.98	-	10.7	36.3	67	6.1	1.04	-	3.0	0.58
2-7	360	26	1260	147	9.1	12.7	6.3	1.78	3.2	11.2	37.4	69	6.7	1.27	-	2.7	0.43
2-8	370	27	1170	135	7.9	12.7	6.2	2.07	2.4	11.0	38.0	72	6.5	1.19	1.46	3.4	0.43
2-9	380	28	1190	-	7.6	11.1	6.7	2.00	2.7	10.3	36.9	72	6.5	1.11	-	3.4	0.52
2-10	390	29	853	-	7.0	11.8	7.1	1.78	3.2	10.5	37.3	66	6.4	1.25	0.79	2.6	0.51
1-1	400	30	744	119	7.9	12.1	6.9	2.06	2.4	10.7	39.4	71	6.7	1.22	1.30	3.1	0.42
1-2	410	31	644	-	7.5	12.4	7.2	2.36	-	10.4	39.6	74	6.9	1.21	-	3.2	0.45
1-3	420	32	770	116	7.9	11.5	5.9	1.59	2.3	10.3	36.2	67	6.4	1.15	-	4.3	0.51
1-4	430	33	1050	143	8.7	11.6	6.4	1.79	3.0	10.8	36.5	74	6.5	1.19	-	2.9	0.47
1-5	440	34	942	120	8.4	11.5	6.5	1.94	2.4	10.7	37.8	80	6.7	1.27	0.84	3.1	0.56
1-7	460	35	1253	101	7.8	12.6	6.8	1.90	2.3	11.0	38.8	71	6.8	1.29	-	2.8	0.41
1-8	470	36	1207	141	8.2	11.2	6.3	1.58	2.0	10.1	35.4	63	5.8	1.13	0.94	2.5	0.41
1-9	480	37	1330	151	7.9	11.8	5.3	1.78	2.0	10.5	36.0	67	6.3	1.10	-	3.6	0.42
1-10	490	38	995	179	8.4	11.8	6.6	1.88	-	10.5	36.8	72	6.3	1.25	0.90	2.4	0.49
cc-1	500	39	1045	139	7.8	11.9	5.0	1.79	1.6	9.7	32.4	61	5.8	1.01	-	2.6	0.36
cc-2	510	40	936	114	8.1	13.0	6.3	1.76	2.1	9.8	35.2	64	5.9	1.03	-	3.1	0.57
cc-3	520	41	1270	231	9.7	13.3	5.8	1.73	2.7	11.4	36.9	71	6.6	1.33	-	3.5	0.45

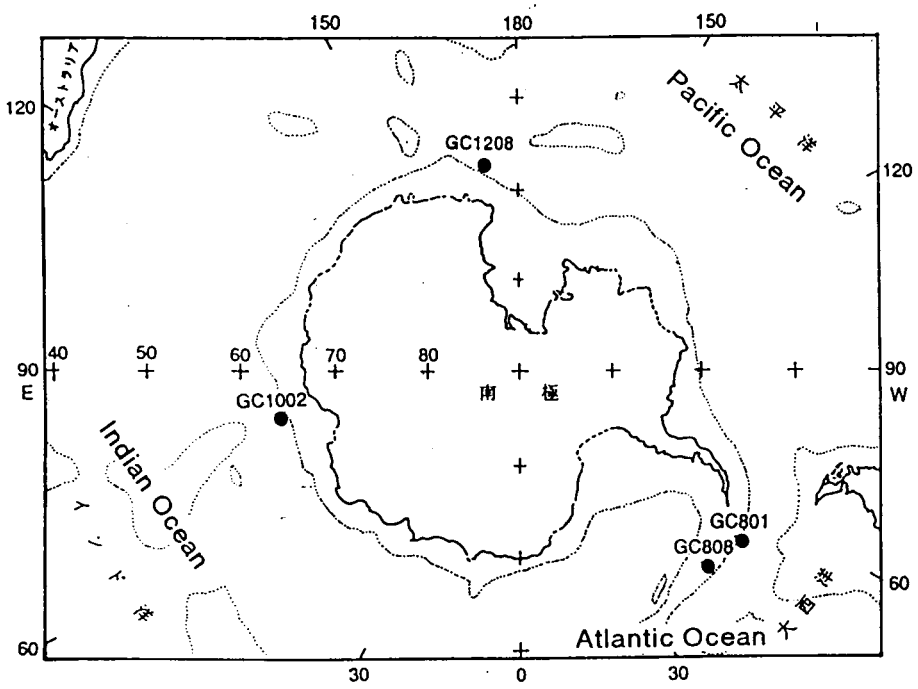

Fig. 1. Topographic map of the Antarctic Ocean and the locations of sediment cores analyzed. Dotted lines show contour lines of 3000m depth.

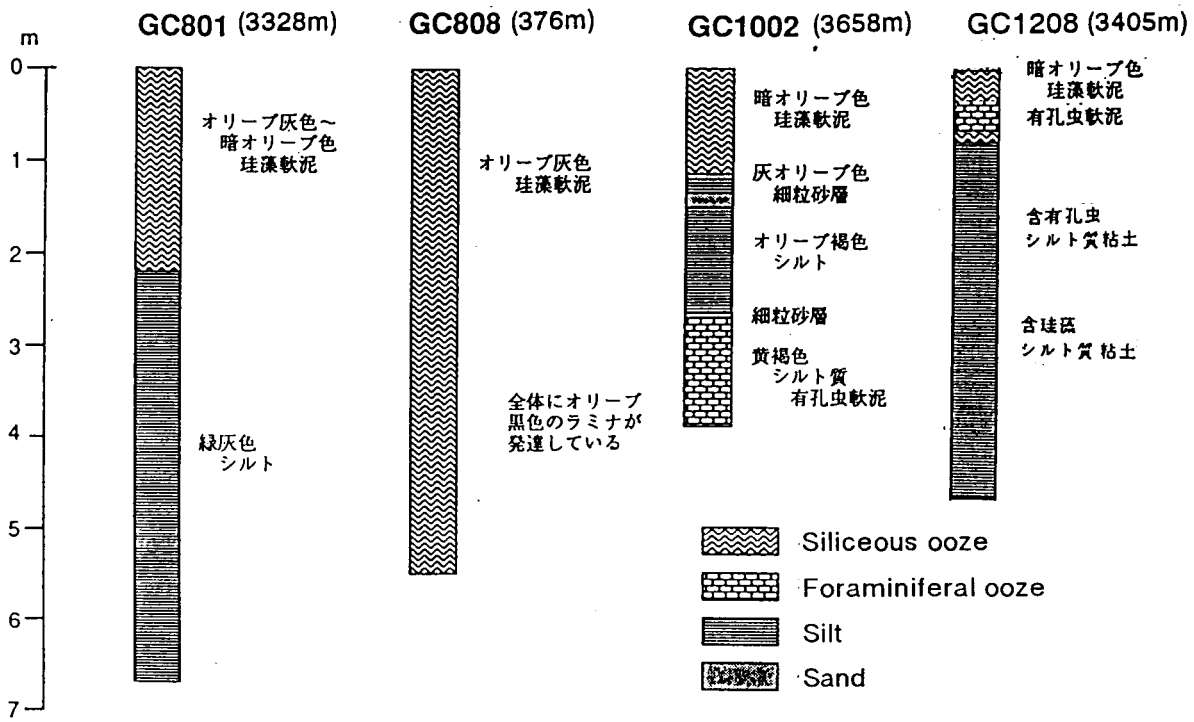

Fig. 2. Lithology of the four sediment cores from the Antarctic Ocean.

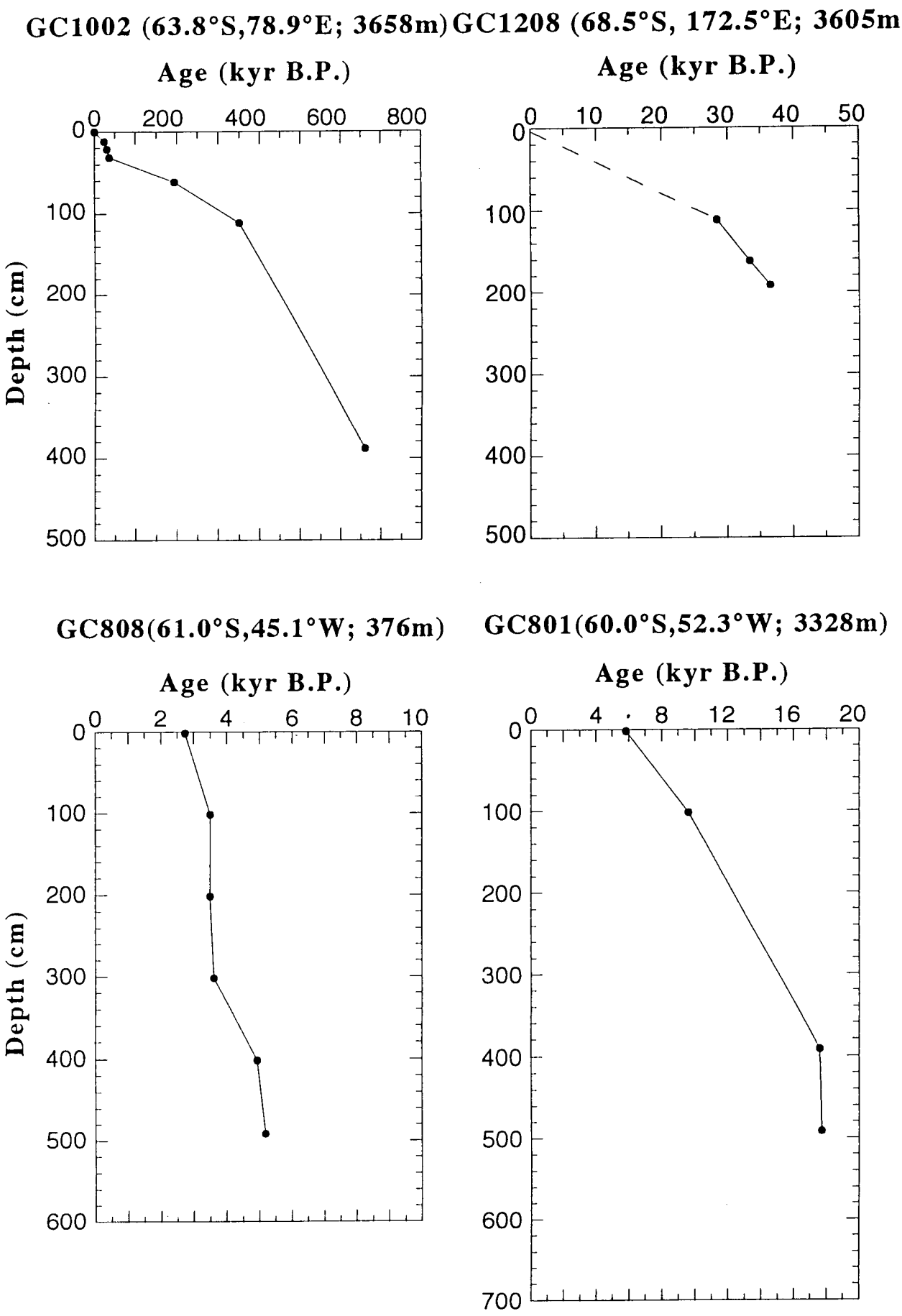

Fig. 3. AMS ^{14}C ages of the four sediment cores from the Antarctic Ocean.

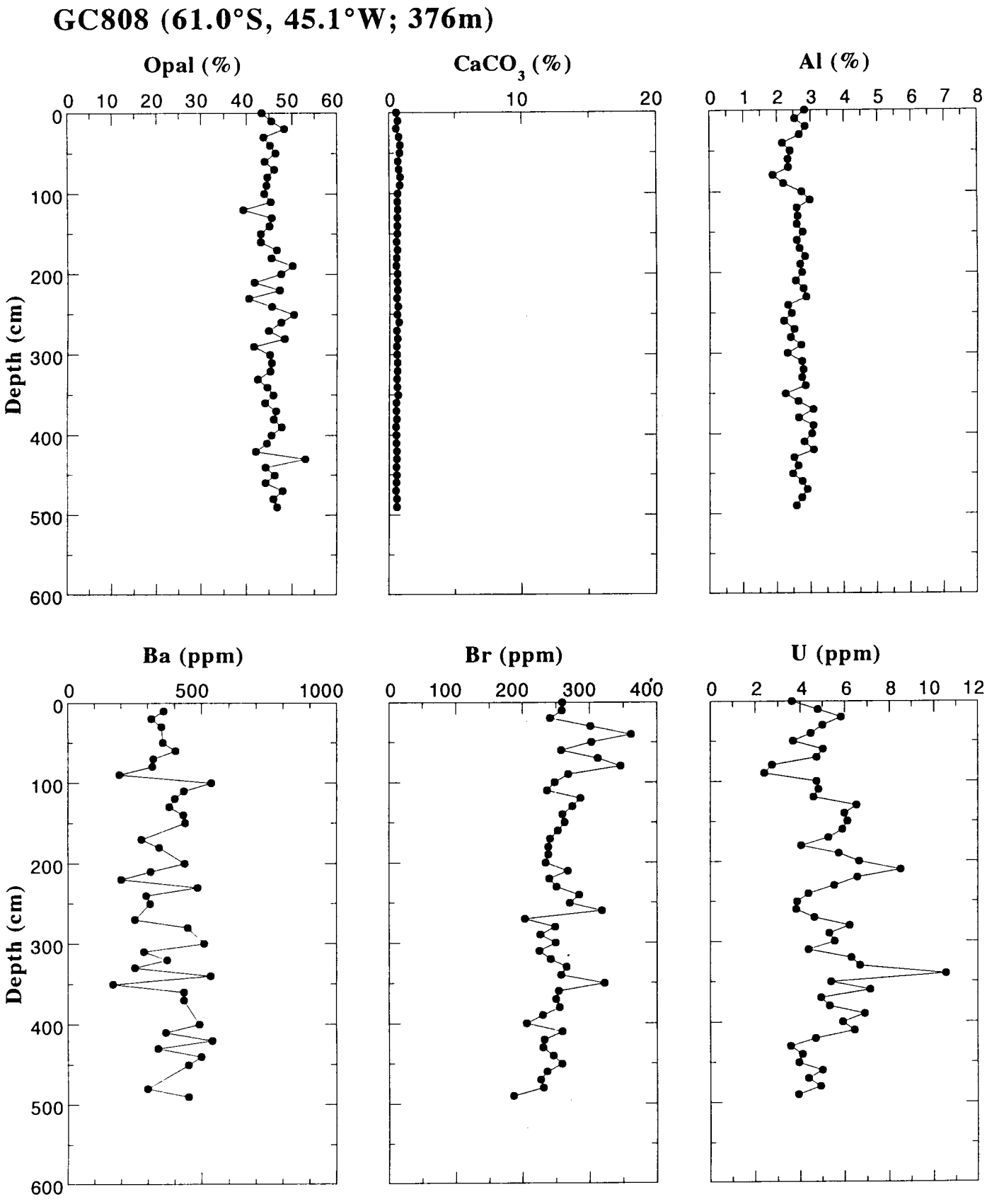

Fig. 4. Vertical profiles of six chemical components in GC 808 Core from the Weddell Sea.

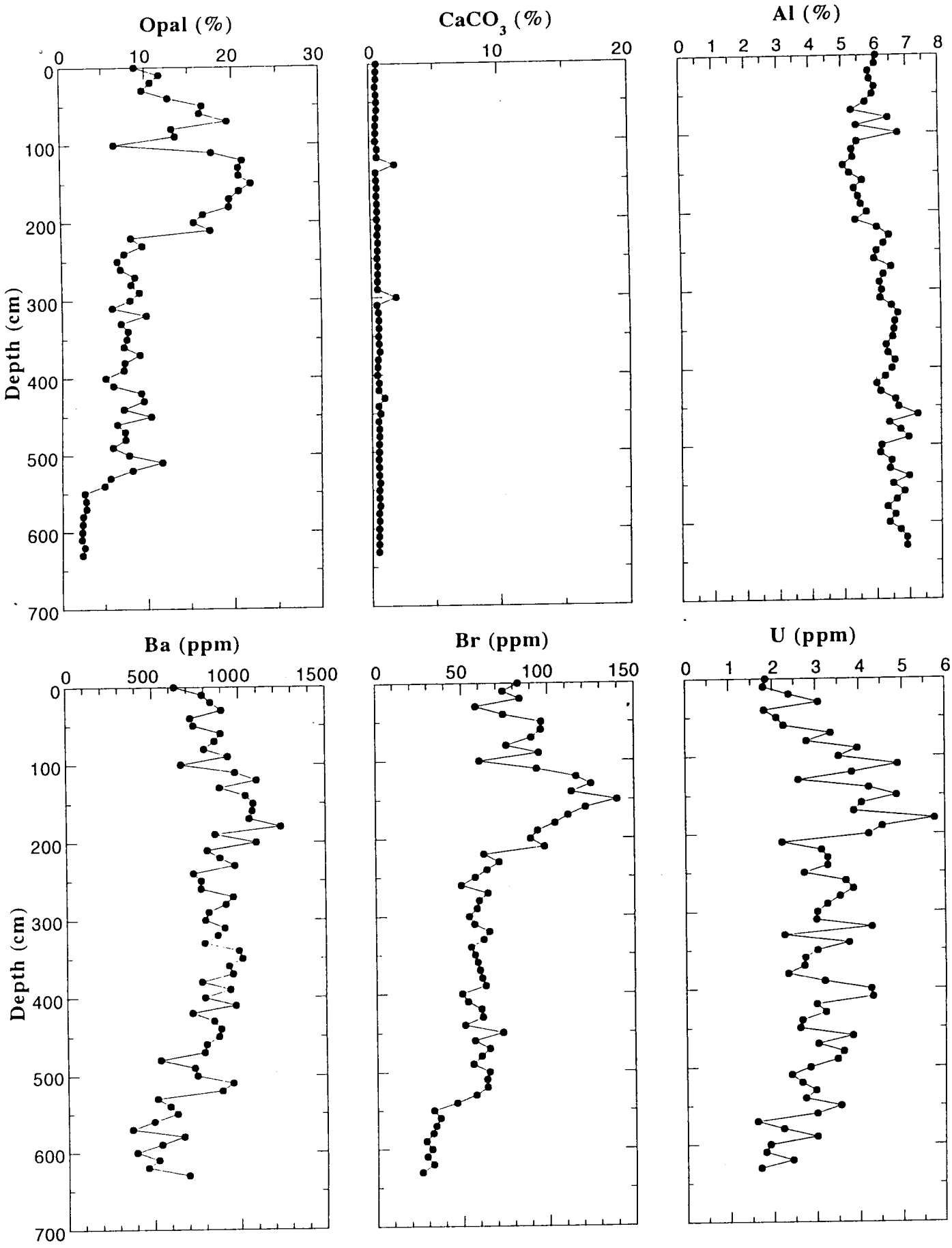

Fig. 5. Vertical profiles of six chemical components in GC 801 Core from the Weddell Sea.

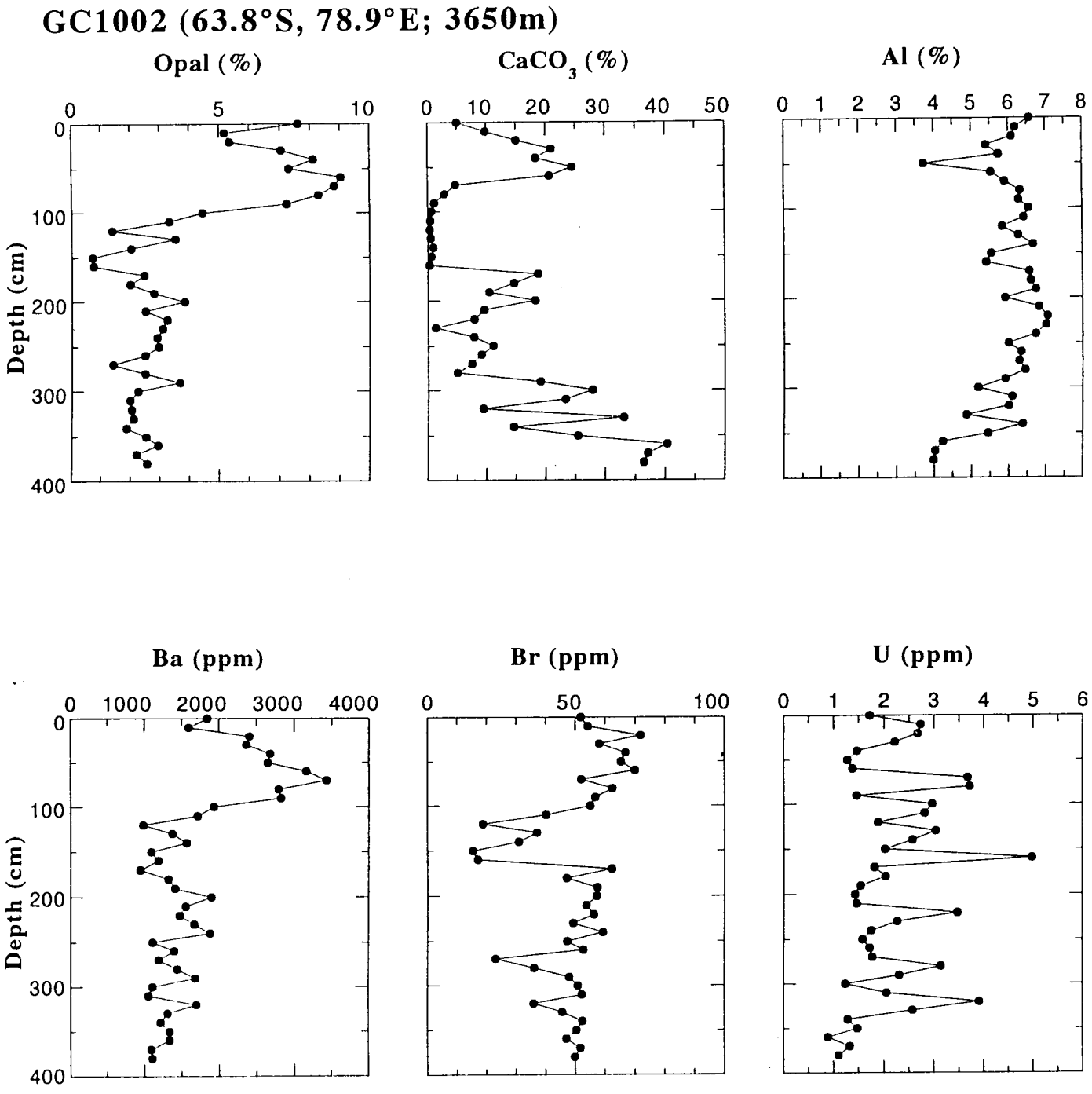

Fig. 6. Vertical profiles of six chemical components in GC 1002 Core from the Enderby Land Basin.

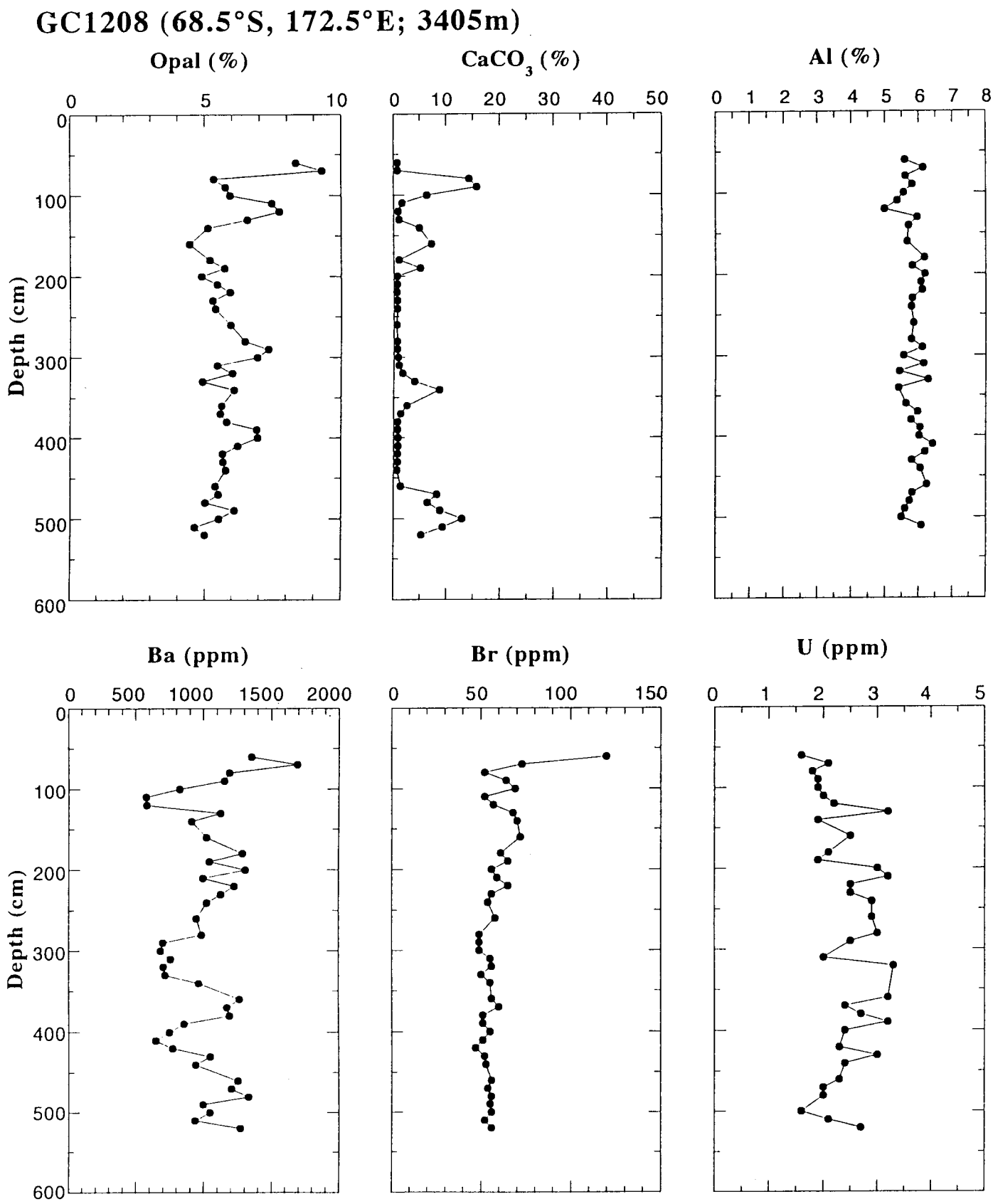

Fig. 7. Vertical profiles of six chemical components in GC 1208 Core from the Ross Sea.

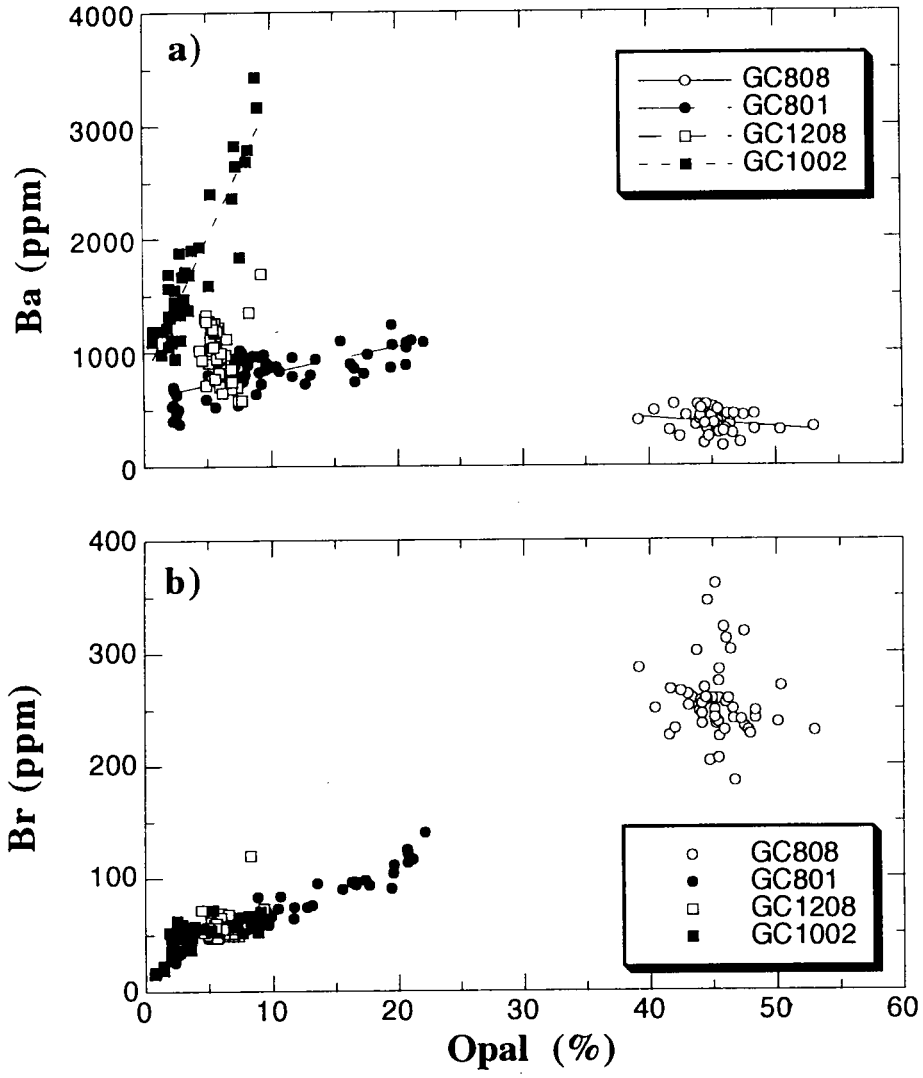

Fig. 8. Relationships of Ba (a) and Br (b) *vs.* opal in four sediment cores from the Antarctic Ocean.

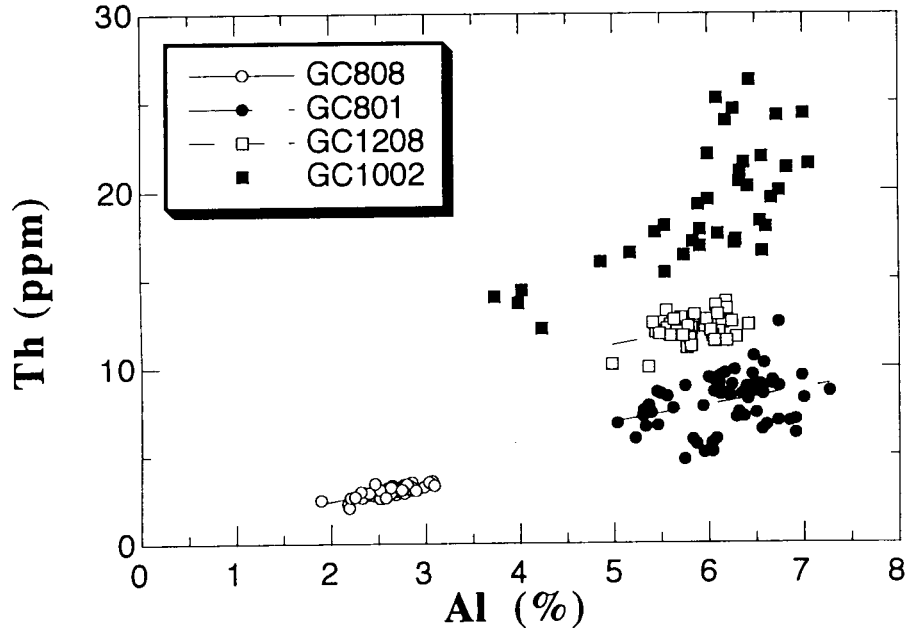

Fig. 9. Relationship between Al and Th contents in four sediment cores from the Antarctic Ocean.